BINARY ASTEROID PAIRS
A Systematic Investigation of the Full Two-Body Problem

Michael Priolo
Jerry Marsden, Ph.D., Mentor
Shane Ross, Graduate Student, Co-Mentor
Control and Dynamical Systems 107-81
Caltech, Pasadena, CA 91125

October 17, 2003

Abstract

We analyze a simple model of binary asteroid pair interaction, the planar restricted full two-body problem. We apply dynamical systems theory to assess equilibrium points and study the phase space near these points. Using analytical and numerical techniques, we locate periodic orbits about the x-axis saddle-center equilibrium points. Currently we are developing numerical methods to catalogue the structure of phase space using the method of Poincaré maps, also known as surfaces of section. A complete investigation of the stable and unstable manifold tubes emanating from the aforementioned periodic orbits will lead to estimations of the collision and ejection rates of binary asteroids.

Contents

1 Introduction to the Binary Asteroid Pair Problem

Three of the twenty-eight known impact craters on Earth are doublets, meaning a binary asteroid pair which hit simultaneously. In fact, approximately 10% of observed near Earth asteroids are

binary. However, planetary scientists cannot fully account for the formation or the evolution of binary asteroid pairs. The binary asteroid pair problem is part of a challenging class of problems in mechanics involving the coupling between rotational and translational degrees of freedom, called "Full Body Problems" (FBPs). FBPs have a wide range of applications including the guidance, control, and dynamics of vehicles, the dynamics of molecular interactions, and the dynamics of celestial bodies. As a first step in understanding the FBP, Jerrold Marsden, professor of Control and Dynamical Systems (CDS) at Caltech and co-workers have begun by analyzing a smaller class of FBPs known as the Full 2-Body Problem (F2BP).[1]

1.1 A Simple Model: The Planar Restricted Full Two-Body Problem

The specific F2BP selected for this study is the planar, restricted, full two-body problem (PRF2BP) developed by Dan Scheeres of the University of Michigan. The model describes the motion of a material point P, in the gravitational field of a massive elliptical body, as shown schematically in Figure 4. The material point has no effect on the massive body. The normalized equations of motion for a frame co-rotating with the asteroid are

$$\begin{aligned} \dot{x} &= v_x \\ \dot{y} &= v_y, \\ \dot{v_x} &= 2\dot{v_y} - \frac{\partial U}{\partial x} \\ \dot{v_y} &= -2\dot{v_x} - \frac{\partial U}{\partial y}, \end{aligned} \tag{1}$$

where

$$\begin{aligned} U(x,y) &= -\frac{1}{\sqrt{x^2+y^2}} - \frac{1}{2}(x^2+y^2) + U_{22}, \\ U_{22} &= -\frac{3C_{22}\left(x^2-y^2\right)}{\left(x^2+y^2\right)^{5/2}}. \end{aligned}$$

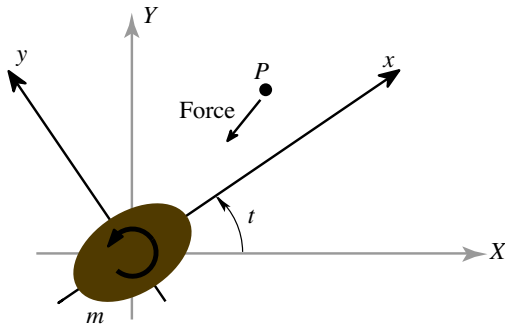

Figure 1: **Simple illustration of the PRF2BP.** The key features include the x and y axes of the rotating frame, the elliptical central mass, and the travelling material point P.

This system has one free parameter, the gravitational field coefficient, $C_{22} = \frac{1}{20}(1-\beta^2)$, having a value between 0 and 0.05. The unit of length is the long axis of the ellipse. The short axis of the ellipse is $\beta \leq 1$. The unit of time is $\frac{1}{2\pi}$ of the rotation period of the asteroid. The C_{22} coefficient is referred to as the ellipticity of the central body. Thus, at $C_{22} = 0$, the system simplifies to the planar, Kepler problem, wherein a material point feels the gravitational attraction of a massive, spherical body at the origin.

2 Analysis of the PRF2BP

In order to understand the dynamical process leading to collision and ejection of material points traveling near the asteroid, we first find a corridor that allows passage between realms. The interior realm is a region of phase space near the asteroid which has a complete boundary when the energy of the system,

$$E = \frac{1}{2}(v_x^2 + v_y^2) - U(x,y) \tag{2}$$

dictated by the equations of motion, is below a threshold value E_s. The boundary can itself be an appreciable section of space, and outside of this barrier is the exterior realm (see Figure 2). Transport between these realms is mediated by cylindrical invariant manifolds emanating from periodic orbits around the x-axis equilibrium points of the system. Therefore, the order of analysis is as follows: first, we discuss how the equilibrium points are found; second, phase space near these fixed points is studied; third, periodic orbits around the equilibrium points are found; and finally, the Poincaré map of the invariant manifolds is numerically constructed.

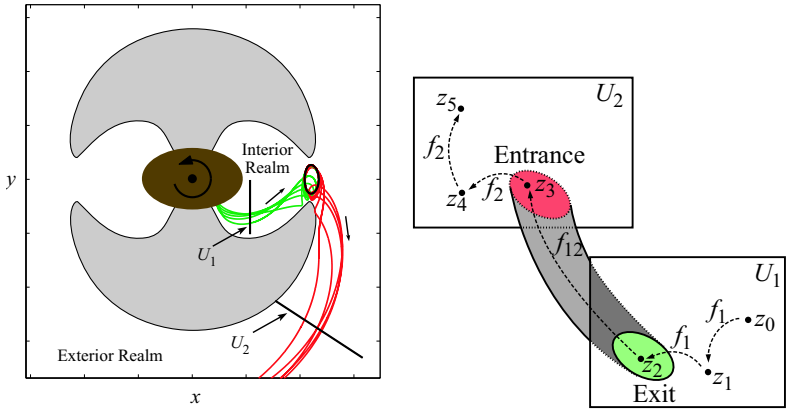

(a) (b)

Figure 2: **Realms of Phase Space and Poincaré Maps.** (a) The enclosed shaded region is the section of position space where the material point cannot travel. This region has a unique shape for different energies of the material point. However, travel between realms is allowed for energies above a threshold, E_s, and occurs through the peroidic orbits on invariant manifolds. (b) U_1 and U_2 are Poincaré maps in phase space that catalogue the trajectories of the manifolds. Illustration used with permission[1].

2.1 Finding Equilibrium Points

Equilibrium points are found[2] at coordinates of position space where both the velocity and the acceleration of the orbiting material point are equal to zero. This corresponds to the point $X = [x\ y\ v_x\ v_y]^T$ of phase space where the right hand sides of the equations (1) vanish. Equilibrium points along the x-axis ($y = 0$) of the rotating frame are located at the real solutions of the following quintic equation,

$$x^2 - |x|^5 + 9C_{22} = 0, \tag{3}$$

and are symmetric about the y-axis. Similarly, along the y-axis ($x = 0$), solutions to

$$y^2 - |y|^5 - 9C_{22} = 0, \tag{4}$$

are equilibrium points, having the same symmetric pair. Solving for these points over a spectrum of $C_{22} \in [0, 0.5]$ reveals the existence of two equilibrium points along the x-axis during the entire spectrum. However, for $C_{22} \in (0, \bar{C_{22}})$, four equilibrium points were found along the y-axis eventually disappearing at $y = \sqrt{15\bar{C_{22}}} \approx 0.74$ (see Figure 3). Along the negative y-axis a pair of equilibrium points approach each other as $C_{22} \to \bar{C_{22}}$, where $\bar{C_{22}} \approx 0.0365$.

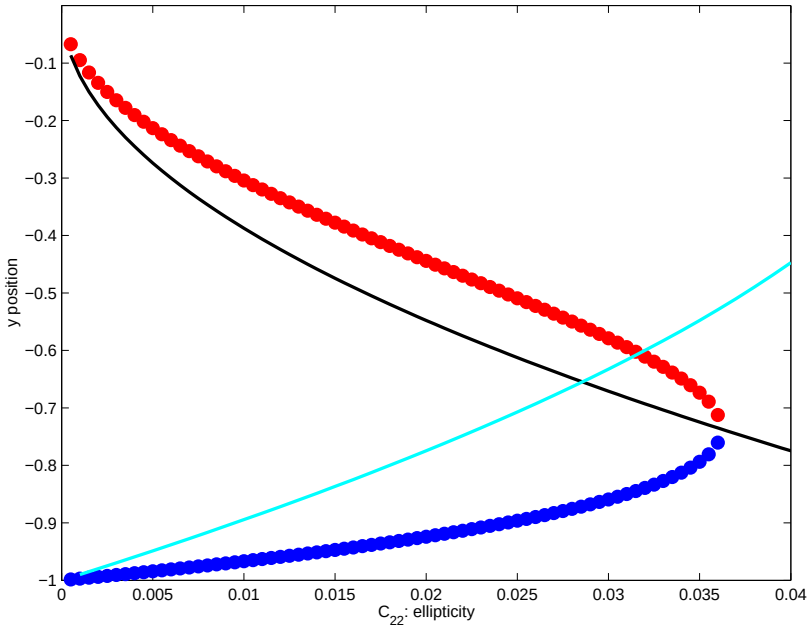

Figure 3: **Convergence and vanishing of equilibrium points.** The solutions to equation (4) above the line $y = \sqrt{15\bar{C_{22}}}$ (the black line), start near the center of the ellipse, and in fact some points lie inside the distance of the semi-minor axis of the ellipse, represented by the cyan line. Material points cannot travel to these points. After this equilibrium point emerges from the asteroid, it soon converges with the second equilibrium point below the line. Location in respect to the line reveals type of geometry of those points.

2.2 Phase Space near Equilibrium Points

Analysis of the four dimensional phase space geometry about these equilibrium points is accomplished through linearization of the equations of motion near those points. Using the first order Taylor formula:

$$f(X) = f(X_0) + Df(X_0)(X - X_0) \tag{5}$$

where X is a vector of parameters and $f(X)$ is a vector of the derivates of the parameters in X:

$$\dot{X} = \begin{pmatrix} \dot{x} \\ \dot{y} \\ \dot{v}_x \\ \dot{v}_y \end{pmatrix}, \tag{6}$$

X_0 is an equilibrium point, and

$$Df = \begin{pmatrix} \frac{\partial f_1}{\partial x} & \frac{\partial f_2}{\partial x} & \frac{\partial f_3}{\partial x} & \frac{\partial f_4}{\partial x} \\ \frac{\partial f_1}{\partial y} & \frac{\partial f_2}{\partial y} & \frac{\partial f_3}{\partial y} & \frac{\partial f_4}{\partial y} \\ \frac{\partial f_1}{\partial v_x} & \frac{\partial f_2}{\partial v_x} & \frac{\partial f_3}{\partial v_x} & \frac{\partial f_4}{\partial v_x} \\ \frac{\partial f_1}{\partial v_y} & \frac{\partial f_2}{\partial v_y} & \frac{\partial f_3}{\partial v_y} & \frac{\partial f_4}{\partial v_y} \end{pmatrix} = \begin{pmatrix} 0 & 0 & 1 & 0 \\ 0 & 0 & 0 & 1 \\ -U_{xx} & -U_{xy} & 0 & 2 \\ -U_{yx} & -U_{yy} & -2 & 0 \end{pmatrix}. \tag{7}$$

Note that $f(X_0) = 0$ and $Df(X_0)$ is constant since particles at the equilibrium point x_0 by definition have no velocity and acceleration. Calculation reveals that $U_{xy} = U_{yx} = 0$ and that U_{xx} and U_{yy} have non-zero values at the equilibrium points. Let $U_{xx}(X_0) = \kappa_1$ and $U_{yy}(X_0) = \kappa_2$. Hence, the matrix of derivatives,

$$K = Df(X_0) = \begin{pmatrix} 0 & 0 & 1 & 0 \\ 0 & 0 & 0 & 1 \\ -\kappa_1 & 0 & 0 & 2 \\ 0 & -\kappa_2 & -2 & 0 \end{pmatrix} \tag{8}$$

leads us to the linearized equations of motion. With a simple coordinate system translation, placing the position space origin at the equilibrium points, the linear equations become the following,

$$\begin{aligned} \dot{x} &= v_x \\ \dot{y} &= v_y \\ \dot{v_x} &= -\kappa_1 x + 2v_y \\ \dot{v_y} &= -\kappa_2 y - 2v_x \end{aligned} \tag{9}$$

2.3 Eigenvalues and Eigenvectors

Additional information about the system is found in the eigenvalue analysis of the matrix of partials, matrix K. The four eigenvalues take the following form,

$$\lambda = \pm\sqrt{-\kappa_1}, \pm\sqrt{-\kappa_2}. \tag{10}$$

Whether these eigenvalues are all real, all imaginary, or a pair of both reveals the geometry of the phase space near the equilibrium points. Therefore, the sign of the κ values is worth investigating. Until now, the equilibrium points on both axes have been denoted by X_0. Let solutions to the quintic equation (3) be $a = (x_{eq}, 0, 0, 0)$ and the solutions to equation (4) be $b = (0, y_{eq}, 0, 0)$. Corresponding κ_i values shall be represented by α_i for a and β_i for b where $i = 1, 2$. Their values are as follows,

$$\begin{aligned}
\alpha_1 &= -\frac{2}{|x_{eq}|^3} - 1 - \frac{36C_{22}}{|x_{eq}|^5}, \\
\alpha_2 &= \frac{1}{|x_{eq}|^3} - 1 + \frac{21C_{22}}{|x_{eq}|^5}, \\
\beta_1 &= \frac{1}{|y_{eq}|^3} - 1 - \frac{21C_{22}}{|y_{eq}|^5}, \\
\beta_2 &= -\frac{2}{|y_{eq}|^3} - 1 + \frac{36C_{22}}{|y_{eq}|^5}
\end{aligned} \tag{11}$$

Clearly $\alpha_1 < 0$ for all C_{22}, and it can be shown that for $C_{22} > 0, \alpha_2 > 0$. Hence, the two equilibrium points on the x-axis have a pair of real eigenvalues and a pair of complex eigenvalues. This is characteristic of a *saddle-center* geometry. On the other hand, while it also can be shown that for $C_{22} > 0, \beta_1 < 0$, the sign of β_2 depends on a relationship between the location of the equilibrium points and the parameter C_{22}. When

$$|b| < \sqrt{15C_{22}}, \beta_2 > 0, \text{a pair of complex eigenvalues;} \tag{12}$$

$$|b| = \sqrt{15C_{22}}, \beta_2 = 0, \lambda = 0; \tag{13}$$

$$|b| > \sqrt{15C_{22}}, \beta_2 < 0, \text{a pairs of real eigenvalues;} \tag{14}$$

The third condition reveals C_{22} values that give rise to two pairs of real eigenvalues which describe the a saddle-saddle point, a geometry with extreme instablity. As shown in Figure 3, the two equilibrium points approach each other and vanish when $|b| = \sqrt{15C_{22}}$.

2.4 Finding Periodic Orbits

Saddle-center geometries have directions of instability as well have trajectories about their centers that are neither stable nor unstable[2]. These paths are periodic orbits around the equilibrium points. One way to find periodic orbits is to choose an initial condition near a saddle-center equilibrium point in the center subspace spanned by the two eigenvecotrs belonging to the imaginary eigenvalues. Then, one numerically integrates the trajectory, and continues to slightly modify the initial condition until the trajectory arrives back on itself.

2.5 Poincaré Map of Invariant Manifold Tubes

Once a periodic orbit is found, we follow the points along the unstable manifolds emanating from the periodic orbits by adding a small scalar multiple of the eigenvectors of the complex eigenvalues which correspond to the directions of the unstable manifolds[2]. These manifolds are cylindrical and two-dimensional winding through the three-dimensional energy surface. Poincaré mapping allows for cuts at different sections of the manifolds to be mapped in phase space (see Figure 2(b).

3 Results and Conclusion

Most of the time invested in this project was spent developing sophisticated numerical algoriths to produce the Poincaré maps. Earlier version of the simulator program produced maps similar to the maps made by Dan Scheeres in his pilot study. However, the full simulator code needed to track the invariant manifolds is not yet operational.

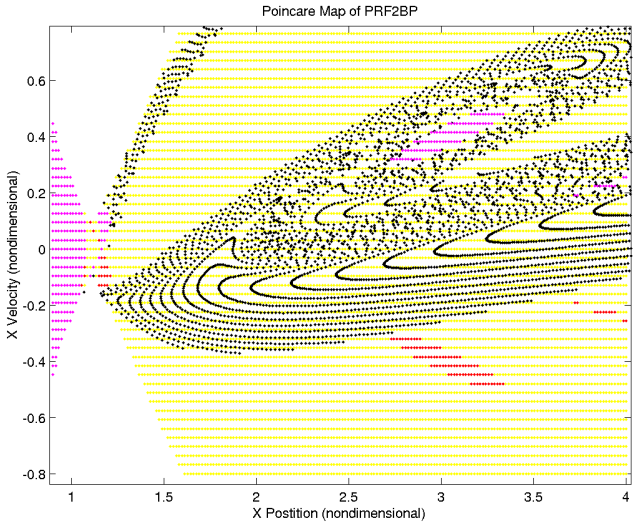

Figure 4: **Poincaré Map Revealing Collision and Ejection Regions.** Regions of phase space that lead to collision and ejection are shown by the red points. Yellow points represent initial conditions while the black points show where in phase space the initial conditions intersect the map.

3.1 The Future of the Binary Asteroid Pair Problem

The binary asteroid pair problem has received much attention in the last couple years, and scientist will continue to modify their models and enhance their computing capabilities to acheive better understanding. Members of the NAST group are currently looking into two areas to better simulate this interaction. First, upon completion of this part of the project, Additional geometric properties, the actual shape and size of the ellipse in the PRF2BP, will restrict the trajectories of the material points and allow for the simulation of elastic and inelastic impacts with the asteroid surface. Second, numerical results and more advance methods, including sympletic and variational integrators, will

be compared against traditional Runge-Kutta schemes. Furthermore, we could develop a kinetic theory of ejection and collision rates of material poits, using ideas from computational chemistry[3].

4 Acknowledgements

This research could not have been possible without my helpful colleagues, friendly summer students and faculty, and generous funding. I would like to thank Shane Ross, my co-mentor, who sparked my interest in this study and brought guidance to my work. I would like to thank the rest of the NAST group and my mentor, Jerry Marsden for their thoughts and expertise that they provided whenever I needed it, especially when I did not know that I needed it. I am exteremely grateful to the handful of computer science undergraduates whose programming ability far surpass mine. Lastly, I extend my appreciation to Mr. and Mrs. Clyde C. Chivens, the SURF Fellows who graciously funded my research.

References

1. Koon, W. S., J. E. Marsden, S. D. Ross, M. W. Lo and D. J. Scheeres [2003] Geometric mechanics and the dynamics of asteroid pairs. *Annals of the New York Academy of Sciences*, to appear.

2. Koon, W. S., M. W. Lo, J. E. Marsden and S. D. Ross [2003] *Dynamical Systems, the Three-Body Problem, and Space Mission Design*, preprint.

3. De Leon, N. [1992] Cylindrical manifolds and reactive island kinetic theory in the time domain. *J. Chem. Phys.* **96**(1), 285-297.